

High-Pressure Phase Equilibrium and Raman Microprobe Spectroscopic Studies on the CO₂ Hydrate System

Shinya Nakano, Masato Moritoki, and Kazunari Ohgaki*

Division of Chemical Engineering, Graduate School of Engineering Science, Osaka University, Toyonaka, Osaka 560-8531, Japan

The three-phase coexistence curve of CO₂ hydrate + saturated water + saturated liquid CO₂ was investigated in the temperature range from 289 to 294 K and pressure up to 500 MPa. The temperature maximum point on the equilibrium curve was confirmed at 294 K and 328 MPa. The sign of (dp/dT) of the three-phase coexistence curve changes from positive to negative at this boundary point. The equilibrium curve continues up to the four-phase coexistence point, which lies at a slightly higher pressure than that of melting curve of CO₂. The laser Raman microprobe spectroscopic analysis reveals that the stretching and bending vibration energies of CO₂ entrapped into the hydrate cage are lower than that of pure CO₂ at the same temperature and pressure. The Raman spectrum for the intermolecular vibration mode (O–O stretching) of water molecules was detected around 200 cm⁻¹ in the hydrate phase. The pressure dependence of the Raman shift reveals that the hydrate lattice constructed of water molecules is shrunk by a pressure increase. The Raman spectroscopy suggests that the hydrate-cage-like structure is provided previously in the aqueous solution in equilibrium.

Introduction

The global greenhouse effect of CO₂ has attracted much attention as a worldwide problem. The idea of CO₂ storage on the ocean floor and natural-gas exploitation in linkage with CO₂ isolation under the deep ocean floor has been proposed lately as methods for holding the CO₂ concentration below a given level (Ohgaki et al., 1996, 1997). In both the ideas, the hydrate crystal of CO₂ could play an important role in preventing anthropogenic CO₂ from entering the atmosphere because CO₂ reacts with water to form the CO₂ hydrate in the temperature and pressure conditions of the deep ocean.

The three-phase coexistence data for the CO₂ hydrate system have been reported as the stability boundary of CO₂ hydrate by many investigators, and they were compiled in texts (Berecz and Balla-Achs, 1983; Sloan Jr., 1990). However, most of them correspond to the three-phase coexistence of hydrate (H) + saturated water (L₁) + saturated gas (G) phases between the quadruple points of hydrate (H) + ice (S₁) + saturated water (L₁) + saturated gas (G) and hydrate (H) + saturated water (L₁) + saturated liquid CO₂ (L₂) + saturated gas (G) (Ohgaki and Hamanaka, 1995; Takenouchi and Kennedy, 1964). In the present study, we measured the three-phase coexistence curve of hydrate (H) + saturated water (L₁) + saturated liquid CO₂ (L₂) in the pressure range up to 500 MPa to confirm the stability limit of the CO₂ hydrate system by use of a new apparatus. In addition, the pressure dependence of the intramolecular vibration of CO₂ entrapped in the hydrate cage and the intermolecular vibration of water is analyzed by in situ Raman microprobe spectroscopy.

Materials

Research grade CO₂ of purity 99.99 mol % was obtained from Takachiho Trading Co., Ltd. and used without further

* Corresponding author. FAX: +81-6-850-6268. E-mail: ohgaki@cheng.es.osaka-u.ac.jp.

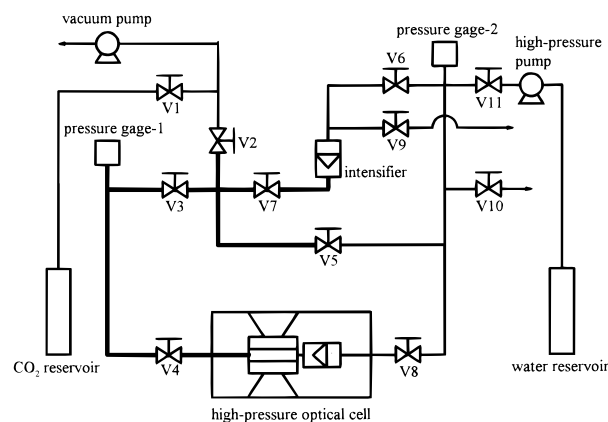


Figure 1. Schematic illustrations of experimental apparatus. V1–V12: valves.

purification. The distilled water was obtained from Yashima Pure Chemicals Co., Ltd.

Experimental Apparatus

The experimental apparatus was designed to prepare single crystals of gas hydrates and moreover to perform in situ laser Raman spectroscopic analysis. A schematic illustration of the experimental setup built newly in the present study is shown in Figure 1. It consists of an optical high-pressure cell, a high-pressure pump, an intensifier, pressure gauges, temperature-control system, a CCD camera, and a laser Raman microprobe spectrometer.

A cross-sectional view of the optical high-pressure cell is shown in Figure 2. The cell, approximately 0.2 cm³ in volume, was made of heat-treated stainless steel (SUS 630), and the maximum working pressure was about 500 MPa. At the center of the cell a pair of sapphire windows, 5.5 mm thick, was set on the upper and lower sides. For reforming the lattice-defect of sapphire, the upper one having the surface of crystal face (0001) was Hot-Isostatic-

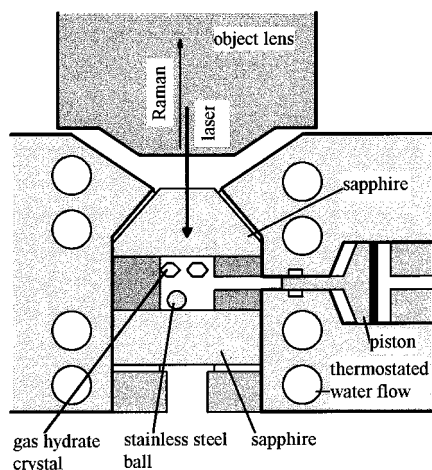


Figure 2. Cross-sectional view of the high-pressure optical cell.

Pressed at ca. 2100 K and 100 MPa by Kobe Steel Ltd. Each window was sealed with a packing made of Teflon type material. The depth and the inner diameter of the inner space were 4.5 and 7 mm, respectively. A stainless steel ball (SUS 304) of 2 mm in diameter was used to agitate the system by vibration generated from the outside. The temperature was controlled by thermostated water flowing out of a thermocontroller (EYELA NCB-3100) into a jacket attached to the cell. The equilibrium temperature was measured within an accuracy of ± 0.02 K by use of a thermistor (Technoseven SXA-33 and D-642-10) inserted into a hole of the cell wall. The contents were pressurized without changing the total amount of substances by use of a volume controller, whose section-area ratio between pressure-increasing water (primary) and sample (secondary) sides was ca. 30:1. The behavior of the inside of the cell was observed by a CCD camera (Shimadzu CCD-F2) through the sapphire window.

The primary water was pressurized by a high-pressure pump (Nihon Seimitsu Kagaku NP-S-252) up to 35 MPa, and further pressurization was performed by the intensifier whose section-area ratio was ca. 20:1. The system pressure up to 500 MPa was measured by a pressure transducer (NMB STD-5000K, pressure gauge-1) and digital peak holder (NMB CSD-819), while the primary water side pressure was measured by a Valcom VPRT-500K (pressure gauge-2) and VPS-A5-350, respectively. The estimated accuracy of the pressure measurement was within ± 1 MPa.

The single crystal of CO_2 hydrate was analyzed by in situ Raman spectroscopy by use of a laser Raman microprobe spectrometer (Jobin Yvon Ramanor T64000) with a multichannel CCD detector. The laser beam for the object lens was irradiated to the sample through the sapphire window. The light source for excitation was an argon ion laser whose wavelength and power level were 514.5 nm and 100 mW, respectively. The Raman ray of the opposite direction was taken in with the same lens.

Preparation of CO_2 Hydrate Crystal and Phase Equilibrium Measurement

A known amount of liquid CO_2 was fed directly from a CO_2 reservoir through the valves 1–4 into the equilibrium cell cooled below 280 K. The ultra purified water was charged from a water reservoir by use of the high-pressure pump up to 35 MPa through the valves 3–5 and 11. At this moment, the interface between the water and liquid CO_2 appeared in the equilibrium cell. Thereafter, the contents were pressurized up to the desired pressure using

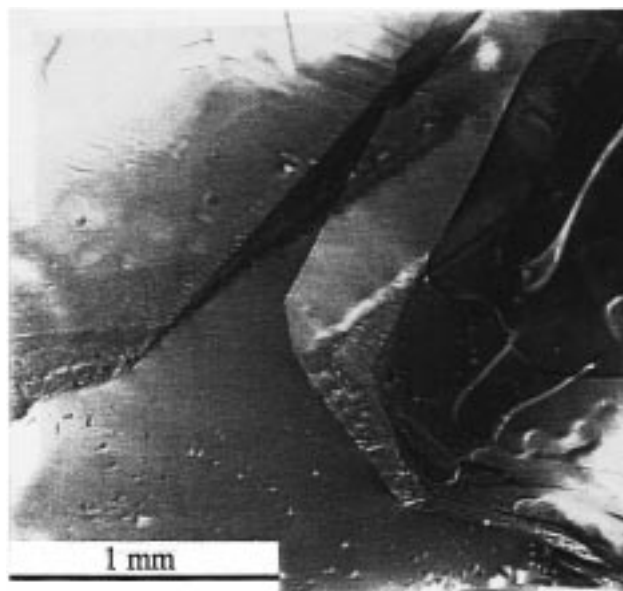


Figure 3. Single crystal of CO_2 hydrate at 292.14 K and 494 MPa. The background is the interface between the saturated water and liquid CO_2 , while the saturated liquid CO_2 lies on the bottom.

the intensifier through the valves 7, 3, and 4 by charging water into the primary compartment of the intensifier through the valves 6 and 11. After the pressurization, the two-phase coexistence state of CO_2 hydrate + water appeared immediately under the conditions of the experiment. Then, the system temperature was increased gradually. The CO_2 hydrate started to dissociate with a rise in temperature, resulting in the appearance of liquid CO_2 particles. Forming and decomposing were repeated by giving perturbations in temperature to remove the hysteresis effect. The contents were agitated intermittently for 24 h so as to establish the three-phase equilibrium. The phase boundaries (liquid + liquid and solid + liquid) were determined by straightforward visual observation using the CCD camera system. When further pressurization without changing the composition of the content was necessary, the cell volume was decreased using the volume controller by charging water into the primary compartment of volume controller through the valves 8 and 11.

In Situ Laser Raman Microprobe Spectroscopy

It is necessary to establish an annealing method for obtaining clear single crystals of CO_2 hydrate for the Raman spectroscopy. The gas hydrate generated in the above experiment was annealed with a temperature cycle method (± 0.05 K one cycle per day) during a few days in the present experiment. In a higher pressure region, quite larger single crystals of CO_2 hydrate formed, usually within 12 h. A typical single crystal of CO_2 hydrate annealed at 292.14 K and 494 MPa is shown in Figure 3. The CO_2 hydrate crystal sinks under the saturated water, and they both float in the saturated liquid CO_2 . In the present experimental conditions, the densities of saturated liquid CO_2 , CO_2 hydrate, and saturated water decrease in that order. With the temperature and pressure kept constant, the single crystal of CO_2 hydrate in equilibrium was put into the laser Raman microprobe spectrometer. The laser beam from the object lens was irradiated to the sample through the sapphire window, and the Raman ray of the opposite direction (the scattering angle was 180°) was taken in with the same lens. The argon ion laser beam was condensed to $2 \mu\text{m}$ in spot diameter, and the spectral

Table 1. Phase Equilibrium Data for Three-Phase Coexistence of CO₂ Hydrate + Water + Liquid CO₂ up to 500 MPa

<i>T</i> /K	<i>p</i> /MPa	<i>T</i> /K	<i>p</i> /MPa
289.73	104	293.97	316
290.32	117	294.0 ^a	328
290.95	138	293.99	338
291.64	158	293.92	358
292.14	177	293.77	377
292.64	197	293.57	397
293.04	218	293.35	422
293.34	237	293.13	441
293.58	257	292.82	460
293.73	276	292.45	479
293.84	296	292.14	494

^a Maximum temperature point.

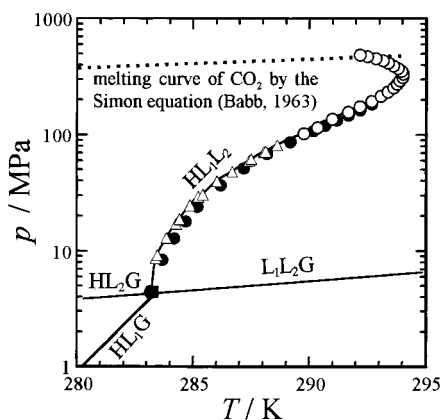


Figure 4. Three-phase coexistence curves of the CO₂ hydrate system: ○, present study; △, Ohgaki (1995); ●, Takenouchi (1964); ■, quadruple point; H, CO₂ hydrate; L₁, saturated water; L₂, saturated liquid CO₂; G, gas.

resolution was about 1 cm⁻¹. The CCD detector was regulated at 140 K for heat-noise reduction. The subtractive spectrograph was calibrated by the Si crystal standard of 520 cm⁻¹. To obtain an adequate S/N ratio, the integration time was varied within the range of 10–300 s depending on the intensity of light scattering, and the average of twice measurements was stored as the spectrum in a personal computer. Neither the laser power below 100 mW nor sampling time (10–300 s) have an effect on the Raman shift in the present conditions.

Results and Discussion

The three-phase coexistence curve (H + L₁ + L₂) obtained in the present study is listed in Table 1 and is shown in Figure 4. One of the most important findings is that the curve has a maximum temperature (294.0 K) at 328 MPa, which means that no matter how high the pressure is raised, CO₂ hydrate cannot exist in the temperature region beyond that temperature. The curve slope dp/dT is negative in the higher pressure region above the maximum temperature point, while the inequality $dp/dT > 0$ holds in the lower pressure region. According to the Clapeyron–Clausius equation, the change in molar volume is consequently the difference between the molar volume of hydrate and that of hydrate former (mixture of the saturated liquid CO₂ and water) at equilibrium T and p . The retrograde point for the SO₂ hydrate system has been also observed in the three-phase coexistence curve (H + L₁ + L₂) by van Berkum and Diepen (1979).

The dotted line in Figure 4 denotes the melting curve of pure CO₂ calculated by the Simon equation (Babb Jr.,

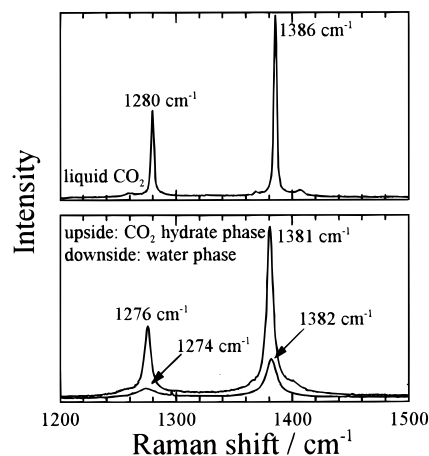


Figure 5. Raman spectra of the CO₂ molecule in the pure liquid CO₂, CO₂ hydrate crystal, and water phase at 100 MPa.

1963). It crosses over the three-phase coexistence curve (H + L₁ + L₂) at 293 K and 474 MPa. The datum point of 500 MPa is the terminal point as far as arriving at the four-phase coexistence point (H + S₂ + L₁ + L₂). The literature values (Ohgaki and Hamanaka, 1995; Takenouchi and Kennedy, 1964) in the low-pressure range are also plotted in Figure 4. The former continuously connects with the present result, while the latter shifts slightly to the higher temperature side. The H + L₁ + L₂ curve originated from the quadruple point (H + L₁ + L₂ + G) had been expected to terminate at the quadruple point (H + S₁ + L₁ + L₂) by Berezic and Balla-Achs (1983). They claimed that the point of intersection of the three-phase equilibrium curve (H + L₁ + L₂) and the melting curve of ice, where H, S₁, L₁, and L₂ are in equilibrium, was a true critical point. However, the present experimental results reveal that the H + L₁ + L₂ curve originated from the quadruple point (H + L₁ + L₂ + G) terminates by way of the retrograde point at the quadruple point (H + S₂ + L₁ + L₂) that lies slightly over the melting curve of pure CO₂. This finding also suggests that the quadruple point (H + S₁ + S₂ + L₁) in the higher pressure region exists slightly over the melting curve of ice.

Typical Raman spectra for the CO₂ molecule are shown in Figure 5 for pure CO₂ (liquid state), CO₂ hydrate, and water (saturated with CO₂) phases. The CO₂ molecule has three normal vibration modes; symmetric stretching vibration mode (ν_1), bending vibration mode (ν_2), and antisymmetric stretching vibration mode (ν_3). Considering the symmetry of the molecule, only vibration mode ν_1 is Raman active while ν_2 and ν_3 are inactive. However, anharmonic coupling between nearly degenerate states of ν_1 and the overtone of ν_2 gives rise to modes ν_+ ($\sim\nu_1$) and ν_- ($\sim 2\nu_2$) in the Raman spectra by the Fermi resonance effect (Wright and Wang, 1973). In the case of CO₂ hydrate, Raman peaks were observed at 1277 and 1381 cm⁻¹, while for liquid CO₂, 1281 and 1386 cm⁻¹, respectively. That is, the spectra of CO₂ in the hydrate phase exhibit shift to the lower frequency side of 4–5 cm⁻¹ than that of the pure state. It means that the CO₂ molecule obtains a considerably wide space compared to the pure state when the water molecules construct a hydrate-cage lattice around it and thus the distance of combination is released.

Moreover, Raman shifts of the CO₂ molecule dissolved in the water phase are very close to those of CO₂ in the hydrate phase. This fact suggests that some hydrate-like structures exist in the water phase; that is, the structure of water around CO₂ in the aqueous solution is similar to

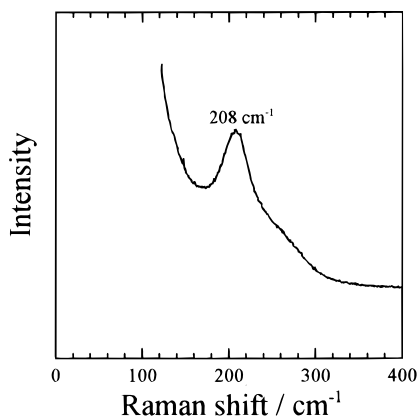


Figure 6. Raman spectra of the intermolecular O–O vibration mode of water in the CO₂ hydrate crystal at 100 MPa.

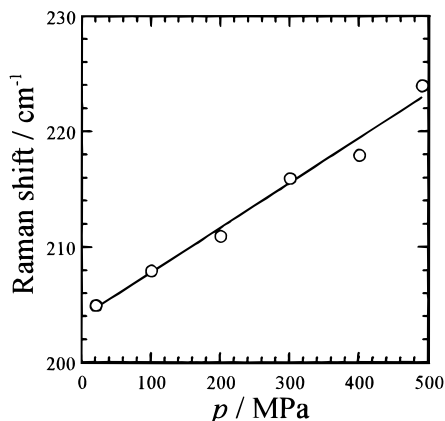


Figure 7. Pressure effect on the intermolecular O–O vibration mode of CO₂ hydrate.

that of the hydrate cage. There is no pressure dependence on the Raman shift of the CO₂ molecule at a pressure range up to 500 MPa in both the hydrate and water phases.

The Raman spectrum of intermolecular O–O vibration mode of water is observed around 200 cm⁻¹ in the CO₂ hydrate crystal as shown in Figure 6. In the hydrate phase, a clear peak is detected on the Rayleigh scattering shoulder. However, no peak is detected in the aqueous solution because the number density of the hydrogen-bonded oxygen is very small in the water phase and the spectrum is hidden in the Rayleigh scattering. The Raman peak of 200 cm⁻¹ corresponding to the hydrate cage structured by hydrogen bonds is a peculiar spectrum of the CO₂ hydrate lattice.

The pressure effect on the O–O vibration mode in the CO₂ hydrate crystal is shown in Figure 7. The O–O vibration energy increases with pressure; that is, the hydrate cage constructed of water molecules shrinks gradually by pressurization. On the other hand, the C–O

vibration energy of CO₂ hydrate is kept almost constant; that is, the cage space is still sufficient for allowing the C–O vibration in the pressure range lower than at least 500 MPa.

Conclusion

The three-phase coexistence curve of CO₂ hydrate + water + liquid CO₂ was obtained up to 500 MPa by use of a newly built high-pressure optical cell with sapphire windows. The retrograde point (maximum temperature point) of the equilibrium curve is confirmed at 294 K and 328 MPa. The single crystal of CO₂ hydrate was analyzed in situ by use of laser Raman microprobe spectroscopy. The stretching and bending vibrations of the CO₂ molecule in both the aqueous solution and the CO₂ hydrate crystal are released by the neighboring water molecules. Also the both Raman peaks have almost the same wavenumber, while the intensities are different from one another. These findings suggest that the hydrate-cage-like structure is provided previously in the aqueous solution in equilibrium.

Literature Cited

- Babb, S. E., Jr. Parameters in the Simon Equation Relating Pressure and Melting Temperature. *Rev. Mod. Phys.* **1963**, *35*, 400–413.
- Berez, E.; Balla-Achs, M. *Studies in Inorganic Chemistry 4; Gas Hydrates, Chapter 3*; Elsevier: New York, 1983.
- Ohgaki, K.; Hamanaka, T. Phase-Behavior of CO₂ Hydrate–Liquid CO₂–H₂O System at High Pressure. *Kagaku Kogaku Ronbunshu* **1995**, *21*, 800–803.
- Ohgaki, K.; Takano, K.; Sangawa, H.; Matsubara, T.; Nakano, S. Methane Exploitation by Carbon Dioxide from Gas Hydrates—Phase Equilibria for CO₂–CH₄ Mixed Hydrate System. *J. Chem. Eng. Jpn.* **1996**, *29*, 478–483.
- Ohgaki, K.; Nakano, S.; Matsubara, T.; Yamanaka, S. Decomposition of CO₂, CH₄ and CO₂–CH₄ Mixed Gas Hydrates. *J. Chem. Eng. Jpn.* **1997**, *30*, 310–314.
- Sloan, E. D., Jr. *Clathrate Hydrates of Natural Gases*; Dekker: New York, 1990.
- Takenouchi, S.; Kennedy, G. C. Dissociation Pressures of the Phase CO₂·5.75H₂O. *Geol. Notes No. 293*; Institute of Geophysics, University of California, Berkeley, 1964; pp 383–390.
- Uchida, T.; Takagi, A.; Hirano, T.; Narita, H.; Kawabata, J.; Hondoh, T.; Mae, S. Measurements on Guest–Host Molecular Density Ratio of CO₂ and CH₄ Hydrates by Raman Spectroscopy. *Proc. 2nd Int. Conf. Natural Gas Hydrates* **1996**, 335–339.
- van Berkum, J. G.; Diepen, G. A. M. Phase Equilibria in SO₂ + H₂O: The Sulfur Dioxide Gas Hydrate, Two Liquid Phases, and the Gas Phase in the Temperature Range 273 to 400 K and at Pressures up to 400 MPa. *J. Chem. Thermodyn.* **1979**, *11*, 317–334.
- van der Waals, J. H.; Platteeuw, J. C. Clathrate Solutions. *Adv. Chem. Phys.* **1959**, *2*, 1–57.
- Wright, R. B.; Wang, C. H. Density Effect on the Fermi Resonance in Gaseous CO₂ by Raman Scattering. *J. Chem. Phys.* **1973**, *58*, 2893–2895.

Received for review February 24, 1998. Accepted May 25, 1998. This research was supported in part by the Kansai Electric Power Co., Inc. (The Kansai) and the Institute for Laser Technology. The authors are also grateful to Department of Chemical Engineering, Osaka University, for the scientific support by "Gas-Hydrate Analyzing System (GHAS)".

JE9800555